Inertia and Frequency Support From Britain's AC Powered Trains

Callum Henderson , *Student Member, IEEE*, Agusti Egea-Alvarez , *Member, IEEE*, Joan Rull-Duran, Marcel Nedd, Panagiotis N. Papadopoulos , and Lie Xu , *Senior Member, IEEE*

Abstract—The penetration of converter connected generation is increasing globally, bringing with it valid concerns over the stability of the modern electricity network. In terms of frequency stability, the provision of inertia and frequency support from converter interfaced generation has been the topic of significant research with a wide range of systems considered. One resource that has avoided significant attention is the GB rail electrical rolling stock. Everyday thousands of trains run on a strict schedule, travelling at high speeds with considerable mass all acting as one large energy store. The AC connected trains possess regenerative braking systems allowing for this energy to be harvested. With simple software modifications this energy can be extracted during large frequency events. This article investigates the power available for inertia and frequency response throughout a working day. A sensitivity analysis of parameters is conducted and the work looks to the future by considering increasing penetration of AC trains. A response between 300–850 MW is estimated for a one-minute frequency response. The calculated energy and response profile was then used to investigate the effect that the trains would have had on the 9th of August power cut that occurred in the U.K. in 2019.

Index Terms—Railway engineering, energy Storage, power system stability, frequency response, inertia.

I. INTRODUCTION

ON THE 9th of August of 2019, there was a power-cut that affected 1.1 million consumers in Great Britain including private customers and critical infrastructures [1]. One of the most affected services was the national railways where

hundreds of train services were cancelled across the country. During the event, several power stations went offline and the low-frequency demand disconnection (LFDD) was activated for the first time in 11 years [2]. Considering the events, alternative methods to support the grid frequency should be investigated. As more converter interfaced generation is connected to the power system, the available network inertia is expected to continue declining [3]. Several power system operators worldwide have expressed concerns that this might cause the system to become unstable [4], [5].

Remedial action, such as inertia and enhanced frequency response from unconventional sources such as batteries [6], electric vehicles [7], [8] and wind turbines [9], [10] has been suggested. The goal of these systems is to support network in the minutes directly following a frequency event to provide time for secondary and tertiary frequency responses to activate. In light of the challenging situation regarding frequency stability, National Grid ESO has started the trial of a new market-oriented service for the provision of inertia from synchronous and non-synchronous equipment [11]. Presently, the railways are not included. However, the service could be included using a similar regulatory framework to those already suggested for other, alternative sources of inertia support (IS) and frequency support (FS). This paper reflects on the idea of railways playing a more active role in power system operation. Especially in the case of large frequency imbalances that might lead to a blackout. Trains are usually seen as a load, but their large inertia and regenerative braking systems make them capable of providing short-term power to the grid with minimal impact on the service schedule, safety and passenger comfort.

Modern AC electric multiple-units (EMUs) are interfaced with a power converter that decouples the grid dynamics from the EMU power train dynamics and allows regenerative braking [12]. This means that the modifications required to provide frequency support can be reduced to software modification. The grid-side converter already utilises a measure of frequency for dynamic synchronisation with the grid. Hence, an extra control loop can be added making the regenerative brake sensitive to this pre-existing electrical frequency measurement under large disturbances, similar to the already suggested frequency support loops for wind turbines [10]. The train converter as well as the railway substation ratings and spacings are already designed accounting for bi-directional power flow from the regenerative braking system which the proposed system will not exceed. Additionally, the traction substations are designed to

cope with overloads for some minutes [13]; BS EN50329:2003 states that mainline railway traction transformers should be able to withstand 3 p.u. current for 300 seconds [14]. Moreover, EN50388:2012 governs the interoperability of the railway network, including the action of the regenerative braking systems. The provision of IS and FS is unlikely to violate these standards [15]. At the same time, railway protection and signalling systems are designed to deal with small speed deviations [16] such as the ones introduced by the provision of IS and FS. Further to this, the system will only activate on rare occasions in the presence of extreme frequency events, once or twice a year as an absolute maximum and probably less. Hence, normal railway operation will continue for the most part. Once the electrical frequency has returned to normal values or the EMU has delivered all the power above a threshold, the train can start to motor again or can continue coasting to allow the power system to recover. AC EMUs are a single-phase load but mitigation techniques such as the V, Scott or Le Blanc connection are applied to ensure a balanced distribution [17]. These methods have been widely researched over the past three decades [18], [19], [20]. Moreover, present research is continuously improving the systems considering the modern network [21], [22]. These techniques should be sufficient to balance the voltage during reversed power flow. Additionally, research on the mitigation of asymmetrical virtual inertia provision from other single-phase systems such as electric vehicle chargers has been conducted which should be applicable for the proposed system [23].

In the GB rail network owned by Network Rail, two main electrification levels exist, 750 V DC in the London area and the south with 25 kV AC supplying the rest of the country [24], [25]. This article focusses only on the provision of inertia and frequency support using AC EMUs as DC-powered rail usually interfaces via a diode rectifier and power reversibility may only be possible with the addition of extra hardware [26]. The instantaneous power that AC EMUs can provide varies from hundreds of kW in regional trains to multiple MW in high-speed (HS) trains during some seconds, depending on the speed.

The article will assess the resource and analyse the impact of using already existing AC EMUs in GB to provide IS and FS during large frequency events. As the train schedule and unit running might suffer modification depending on the day, a probabilistic approach is employed to determine the power that may be available for injection to network. Following this, simulations containing mechanical models of physical train parameters such as inertia, gearing and rolling resistance based on a British Class (BC) 390 are conducted. The model provides insights on how electrical frequency variations affect train speed, acceleration and jerk as well as the support delivered to the electrical network. Another set of simulations using a GB network single bus model will be used to exemplify the impact of the provision of IS and FS from EMUs in a power outage like the one that occurred on the 9th of August 2019.

II. AVAILABLE TRAIN RESPONSE

This section presents the main characteristics of the Britain's AC Network Rail services and estimates the volume of power that may be extracted for IS and FS a base case.
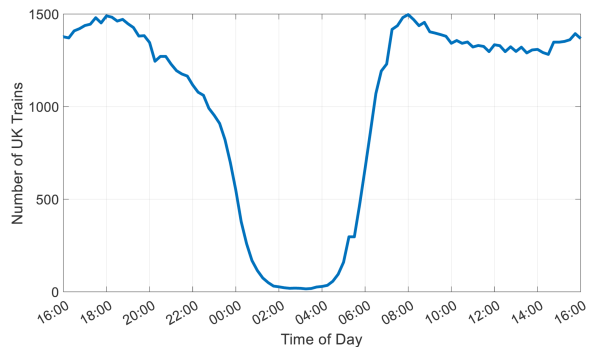
Fig. 1.   U.K. Trains Running During Weekdays.

TABLE I
AC EMU DISTRIBUTION

EMU nominal power, P_{pt} [kW]	EMU type	GB average speed [km/h]	Power consumed at average speed, $P_{average}^{P_{tp}}$ [kW]	Percentage of units in AC EMU GB rolling stock
< 750	CO	54	125	22%
750 – 1,500	RE	98	256	70%
> 3,000	IC & HS	120	845	8%

A. GB Network Rail and Services Taxonomy

The number of trains running in the GB network has been recorded at 15-minute intervals during weekdays using the National Rail data feeds in January 2022 [27]. A plot showing the average number of weekday trains is shown in Fig. 1.

From Fig. 1, 1400 trains run relatively constant throughout the day. Small peaks are observed during rush-hour with a small sag between 9:00 and 16:00. The number of services drops quickly after 19:00 with less than a dozen services running at any time between 1:00 and 4:00. This suggests a predictable and reliable store of power during the daytime when the network is most likely in need of support.

In the GB rail network, around 50% of the services are electric, representing 60% of all passengers [28] and 65% of the electric EMUs are AC [24]. As the GB rolling stock is undergoing a process of modernisation it is expected that all AC EMUs will have regenerative braking capability [29]. Three main categories of EMU in GB are high speed (HS) and intercity (IC), Regional (RE) and Commuter (CO). The distribution of train types and the characteristics can be seen in Table I.

Not all EMUs will be available to provide FS as some of them would run curtailed or would not provide the services for operational reasons. Nevertheless, the FS supplied from the rail network can represent tens to hundreds of megawatts to aid power system stability with a peak during the daytime hours. The amount of running AC EMUs depends on the time and the day of the week. In addition, train speeds can vary considerably and by using a probability density function, a more precise estimate can be made accounting for trains that may be running too slow to provide a response. Moreover, it allows the representation of trains running at high speeds well above the average which is crucial due to the exponential relation between kinetic energy and train speed.

B. Limitations on Power Response

Some considerations must be made when defining the power available for IS and FS. Active power representing synthetic inertia must be delivered quickly, normally within 100 ms and sustained output beyond 10 seconds is not required [30]. The power converter is capable of responding within this time-frame as long as the 1.11.2 p.u. current limit is not exceeded and the application of the regenerative brake at full force would not exceed any limitations on acceleration. The extra current headroom usually required for generators is not necessary as the trains are seen as a load under normal operation. Acceleration of the trains is limited to around 0.37-0.50 m/s^2 for HS/IC EMUs and 1 m/s^2 for RE EMUs [31]. Instead, the first derivative of acceleration (jerk) is a more telling measure of passenger comfort. At high speeds it is unlikely the jerk will pose any issue but may become a factor at lower speeds due to reduced kinetic energy. Hence, the limiting factors are the power converter current rating and the cut-in speed at which trains are allowed to respond. The cut-in speed is defined as the minimum speed the train must be travelling before it is allowed to respond to an event and is determined by the operator. Any train on the network travelling above this speed at the time of an event is allowed to respond. The cut-out speed is defined as the speed where the useable kinetic energy has been depleted after responding to an event. Note that when a train has begun responding, the speed is allowed to fall below the cut-in speed until it reaches the cut-out speed. Most regenerative braking systems cannot provide enough force to brake the train below 20 km/h due to insufficient torque at low speed [32], which provides the physical limit of cut-out speed.

Frequency response must provide a sustained output, in this paper 60 seconds is used as a benchmark to provide the slower primary and secondary responses of power stations time to react [33], [34]. This means that the converter rating is no longer the limiting factor as it is not possible to provide maximum power for such a long period without slowing beyond the cut-out speed. Therefore, the volume of power is determined by the cut-in speed and the maximum allowable speed deviation. In some cases, the maximum speed deviation may be determined by the cut-out speed but for operational reasons it may not be possible to slow the train to the desired extent. An investigation of the effect that different speed deviations have on the power available is conducted in II.C.

C. Probabilistic Distribution of Train Speeds

This subsection describes the speed distribution of the trains used in the study to calculate the IS and FS. As the instantaneous speeds of the trains are not available, a probability density function (PDF) is preferred to determine how many trains are running at each speed. As a predefined PDF for trains services is not available, one is assumed and a sensitivity analysis on the shape and variance parameters is conducted in Section III. This probabilistic approach represents the different states that trains may be in on the network where speeds may be reduced for various external factors. Incline of the railway tracks is not considered as the steepest incline in GB (1 in 37.7) would result in a reduction of available energy of much less than 1% [35].
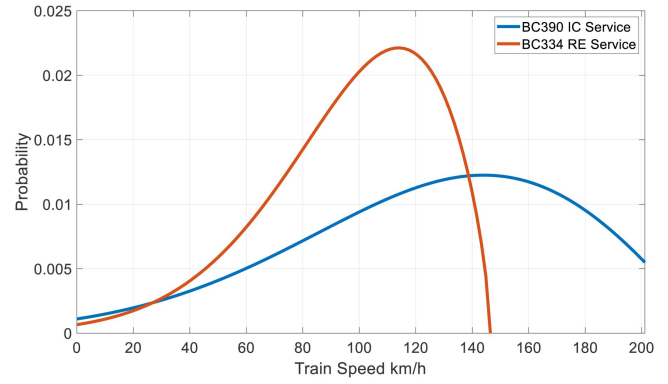
Fig. 2. PDF for Train Speeds.

Since the average speeds of IC and RE trains are larger than half of the maximum speed, a negatively skewed distribution is required with a larger proportion of trains running at higher velocities. The density functions for the IC and RE trains are based on the data in Table I and have a mean speed of 120 km/h and 75 km/h, respectively with a maximum speed of 201 km/h and 145 km/h, respectively. The height of the peak and spread of possible speeds is determined by the variance (σ) of 27 and 18 for the IC and RE, respectively. A skew parameter (k) in both cases is equal to -0.5 and shifts the mode train speed above the average. The IC and RE functions are shown in Fig. 2.

From Fig. 2, both PDFs form a similar shape measured against the respective speed ranges. This is assumed representative of the GB rail network as it is expected a higher proportion of the trains run above the respective average speed. The train speed is unlikely to take on exact integer values, hence the speeds are binned at 2 km/h intervals. The number of trains in each bin are then assumed to run at the middle speed of the bin. The total available energy at 15-minute intervals is calculated as follows by adding the output from the sum of all bins for each of the IC and RE services:

$$E_{kT} = \frac{1}{2}$$

$$\times \left(\sum_{i=1}^{HSb} \phi_{mh}\eta_h m_h n_i \, \delta_v v_{hi}^2 + \sum_{j=1}^{MSb} \phi_{mm}\eta_m m_m n_j \, \delta_v v_{mj}^2 \right) \tag{1}$$

Where E_{kT} is the total energy available from each train type, m_h and m_m are the masses of the IC and RE services, respectively and, n_i and n_j are the number of trains in each bin with i representing the IC bins and j denoting RE bins. v_{hsi} and v_{mj} are then the middle speed of bins i and j converted from km/h to m/s, respectively. HSb and MSb are the number of bins for each respective train service. ϕ_h and ϕ_m are mass factors used to account for the rotational inertia in the drivetrain of the IC and RE services, respectively. η_h and η_m are the regenerative braking efficiencies of each service type, respectively. The parameter δ_v accounts for the percentage the train is allowed to slow during a frequency response:

$$\delta_v = 1 - v_{min}^2 \tag{2}$$

TABLE II
KEY PARAMETER FOR BC334 RE SERVICE AND BC390, IC SERVICE

Parameter	BC334	BC390
Operational Mass (m)	127 t	465 t
Rotational Inertia Mass Factor (ϕ)	1.04	1.06
Top Speed (v_{max})	145 km/h	201 km/h
Regenerative Braking Efficiency (η_b)	80 %	80 %
Converter Power Rating (P_c)	1.5 MW	5.1 MW
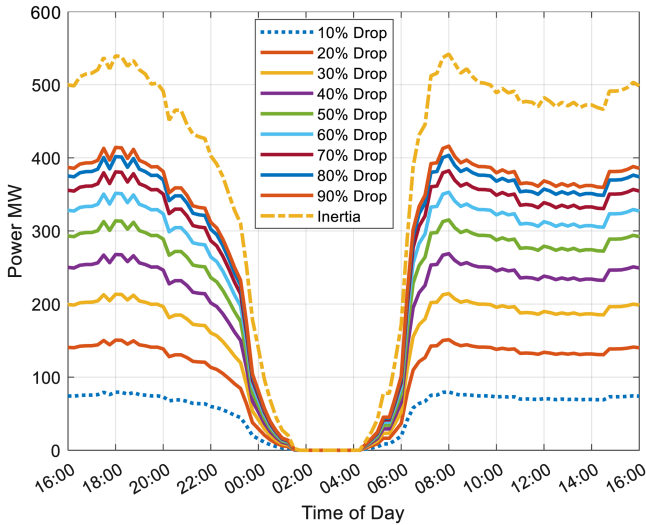
Fig. 3. Predicted 60 second FS and IS available from U.K. Trains.

Where v_{min} is the minimum allowable percentage of the initial train speed as a decimal. The level of frequency response is then calculated assuming the power injection should be sustained for 60 seconds:

$$P_{FS} = \frac{E_{kT}}{60} \quad (3)$$

When considering IS, there is no need to curtail the power output to ensure delivery can occur for 60 seconds. Hence, the power available is then determined by the current limit of the converter, usually 1.2 p.u. [36]. The IS is therefore defined as:

$$P_{IS} = 1.2 I_{cr} V_{cr} \quad (4)$$

Where P_{IS} is the power available for IS and I_{cr} and V_{cr} are the converter current and voltage ratings, respectively.

D. Frequency Response Available

All IC services are based on the representative example of the BC 390 while the RE services are based on the BC 334. These two AC EMUs have very similar speed, weight and power characteristics to other BCs of the same category. Key parameters for BC 334 and BC 390 are listed in Table II.

For both units, a regenerative brake efficiency up to 80% is assumed [32]. The mass factor for BC334 is assumed to be 1.04 as the number of rotating components is reduced compared to BC390 due to the lower numbers of cars. The volume of available power for FS and IS is shown for a weekday for different speed deviations in Fig. 3. The speed deviation is determined

as a percentage of the initial speed. Hence, a 10% drop would indicate the final speed of the train being 90% of the initial speed. For IS, speed deviation is not considered, and the full power of the converter is applied until the train reaches the cut-out speed. A cut-in speed of 40 km/h is used in all cases.

From Fig. 3, at total of over 400 MW is available for FS during peak rush hour times when the maximum speed deviation is used. This ramps off slowly with no notable FS after midnight. Interestingly, if only a 10% speed deviation is used the system can still generate a similar volume of power to a medium sized wind park. The predictability and constant nature of the power source is a large benefit; it is unlikely a large volume of frequency response would be needed between 12:00 and 5:00. It is not efficient to specify an allowable speed deviation above 70% as the energy gain is not sufficient to justify the reduction in train speed.

When considering the IS available using the maximum rating of the converters (yellow dot-dash), an extra 150 MW of power is available compared to the maximum FS for a 90% speed deviation. This power level would be sustainable for around 45 seconds before the physical cut-out speed provided by the regenerative braking would be reached. The time is calculated by dividing the maximum energy available for each train type (totaling ≈ 25.2 GJ) by the respective converter power rating.

III. SENSITIVITY ANALYSES

This section investigates the different sensitivities of the FS and IS to key parameters such as train cut-in speed, train speed distribution and train type distribution. This allows for the determination of the most effective parameters to ensure maximum power extraction at minimal cost to passengers. In addition, the analysis provides an interpretation of the uncertainty surrounding the services with different speed distributions and cut-in speeds representing different rail network conditions.

A. Train Cut-in Speed

The energy available increases exponentially as the train speed rises. Hence, the minimum speed at which the train is allowed to contribute to frequency response is crucial. There is no need to reduce the speed of already slow-moving trains to extract a small amount of energy. The power available for a one-minute frequency response for different cut-in speeds is shown in Fig. 4. The cut-in is measured as a percentage of the maximum train speed to allow the same value to be applied to both service types. A maximum speed deviation of 70% is used in both cases.

From Fig. 4, there is roughly 120 MW between the 70% and 20% responses and no observable difference between the lowest three cut-in speeds. This suggests a 40% cut-in would be the best setting. Setting the cut-in above 70% would result in few trains being capable of contributing to the frequency response. The cut-in speed has a similar effect on the inertia provision as it reduces the probability of services capable of providing a response.
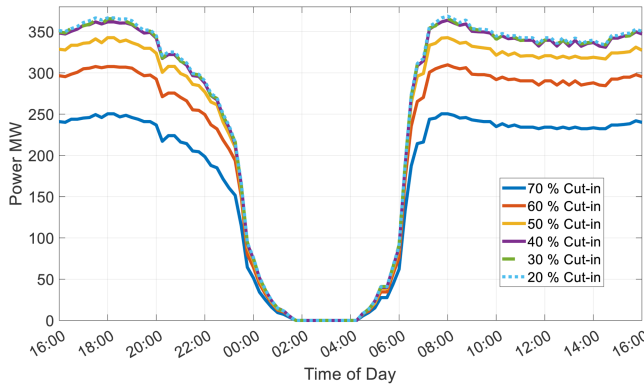
Fig. 4. One minute frequency response for different train cut-in speeds considering a 70% speed deviation.

Fig. 5. (a) Effect of varying distribution parameters on total FR (b) Sensitivity of FR to percentage of electric trains and HS services.

B. Train Speed Distribution

The probability density functions for both train types have been assumed based on the mean train speeds. This means that the distribution must have a negative skew with more trains running at higher speeds. However, this still leaves a large range of possible parameters for the density function. A larger skew with lower variance results in a sharper peak in the HS region between the mean and the maximum. However, this does suggest that more trains run below top speed but still higher than the average. A smaller skew with a larger variance provides a shallower peak with more trains likely to run at the extreme values. This would suggest a higher proportion of trains at a stand-still in stations. As the network rail operation conditions can change depending on several factors (weather, incidents …) the IS and FS estimation should be calculated considering them. Therefore, a range of distributions are considered by varying the skew and variance parameters of the distributions. For example, a more skewed distribution with many trains running at top speed may be representative of a system attempting to recover from delays. Conversely, if more trains run at a slower speed and there is either less skew or variance it may suggest the network is experience operational issues and train speeds are curtailed. A shallow peak with a large variance is likely the distribution during quiet hours when there are less trains on the network. The effect of this on the total power available for a 60 second frequency response is provided in Fig. 5(a). Fig. 5(b) illustrates the sensitivity to electrical train type discussed in III.C. An illustration of the extreme distributions corresponding to the four outer vertices of the grid in Fig. 5(a) is provided in Fig. 6 alongside the speed distribution providing maximum power.

From Fig. 5(a), the skew and variance parameters were each altered by ±50% from the original values. Note that the skew is always negative to maintain a higher proportion of faster trains. A large range of frequency response is available between 250 and 390 MW with the minimum power still representing a large reserve. The increasing magnitude of skew shifts the peak response further to the HS region in some cases increasing the power available. However, in cases where the variance is small this results in the function reaching zero before the top speed is reached. This can be seen in the yellow trace in Fig. 6.
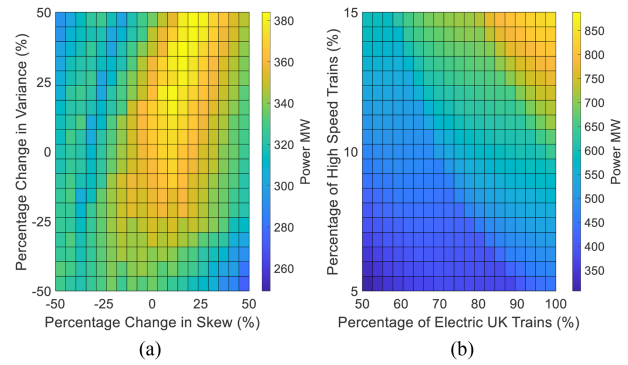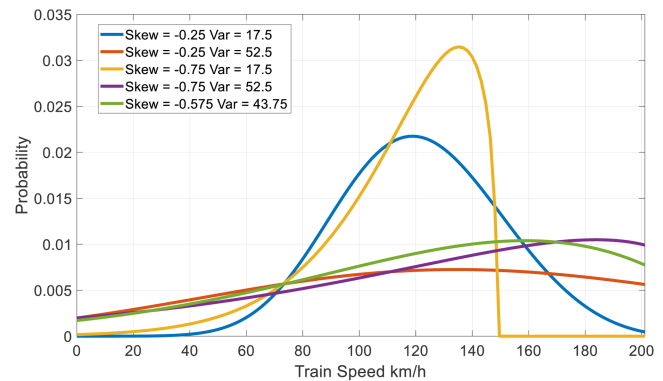
Fig. 6. Extreme and optimal probability density functions.

While this response is unlikely it may occur in extreme weather conditions if services are required to slow. Even if the skew is smaller, a distribution with a small variance is unlikely as this means that no trains will be stopped. This distribution is shown in blue in Fig. 6. It is likely that a higher variance is present in the train speeds allowing for services to be at stand-still or top speed. In these cases, a low skew suggests slightly more running slowly and a high skew indicates a larger proportion running faster. These can be observed by the red and purple traces in Fig. 6, respectively. The PDF providing the largest response is shown in green in Fig. 6. The PDFs shown in Fig. 6 are for the IC services but similar traces are obtained for RE services over a smaller speed range

C. Train Electrical Type Distribution

With the electrification of rail transport set to increase dramatically over the next ten years it is important to consider a different spread of electric versus diesel locomotives. In addition, it is likely that more high-speed services will be added to the system further increasing the available power. This is evident with the HS2 project planned to enter service within the next 10 years [37]. The effect of increasing percentage of electric trains and variation of the proportion of these being high-speed services is shown in Fig. 5(b).

From Fig. 5(b), somewhat obviously, as more GB trains become electric, more energy is available to feed back to the
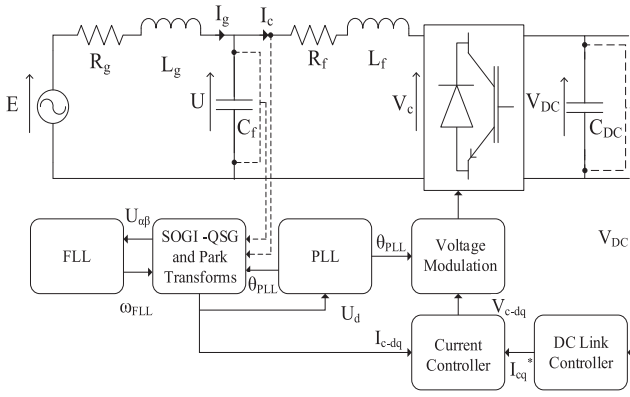
Fig. 7.   Grid-side converter control diagram.

electricity network. Moreover, an increased percentage of heavy, higher power trains also improves the reserve of frequency response. The power is calculated during the busiest time of day and a linear trend is observed in both response to percentage of electric trains and proportion of high-speed services. A massive 890 MW would be available, and this is a conservative measurement since factors like passenger weight are not considered. Assuming that newer services would be faster, more efficient and possess higher power ratings it is easy to see the volume of energy being equivalent to well over 1 GW. However, the available inertia does not form the same trend. Using the same variations, the maximum inertia during peak rush hour was found to be 1.45 GW. Considerably larger than the estimates made in Section II and equivalent to two standard size nuclear power stations with greater dispatchability.

IV. POWER DELIVERY

The exchange of power between the train and electricity network can be achieved via software changes. Moreover, the alteration to the control system can be relatively minor to provide either a frequency or RoCoF dependent power command to the existing control structure. Similar control systems have already been suggested for renewable technologies such as wind farms [10] but could be easily adapted and augmented with systems to ensure the correct operation of the train under normal operating conditions. The controller builds upon work completed in [8], [38].

A. Grid-side Controller

The grid-side converter employs a conventional single-phase current controller. The PCC voltage is fixed to the q-axis and a DC link voltage controller provides the q-axis current command to regulate the flow of active power. No voltage control is present at the PCC in this case and the d-axis current command is left at zero. A control diagram for the grid-side controller is shown in Fig. 7.

The network is modelled using the following equations:

$$sI_g = \frac{E - U}{L_g} + \frac{I_g R_g}{L_g} \tag{5}$$

$$sI_c = \frac{U - V_c}{L_f} + \frac{I_c R_f}{L_f} \tag{6}$$

$$sU = \frac{I_c - I_g}{C_f} \tag{7}$$

Average converter models are utilised and the DC link voltage is generated via a power balance:

$$I_{dc} = \frac{P_n - P_t}{V_{dc}} \tag{8}$$

$$V_{dc} = \frac{I_{dc}}{sC_{dc}} \tag{9}$$

Where I_{dc} is the DC link current and P_g and P_t and the grid and train powers, respectively. A second order generalised integrator with quadrature signal generator (SOGI-QSG) approach is applied:

$$\frac{Y'_\alpha}{Y} = \frac{K_d \omega_c s}{s^2 + K_d \omega_c s + \omega_c^2} \tag{10}$$

$$\frac{Y'_\beta}{Y} = \frac{K_d \omega_c^2}{s^2 + K_d \omega_c s + \omega_c^2} \tag{11}$$

Where Y represents the component being transformed from the single-phase system to the synchronous frame, k_d is a gain term used to adjust the bandwidth of the resonant peak and ω_c is the centre frequency of the filter. This system creates an imaginary phase in quadrature with the original signal in the stationary reference frame. A frequency locked loop (FLL) is used to provide the centre frequency for the SOGI to allow operation across the frequency range:

$$\omega_{FLL} = \frac{K_{FLL} V_e V'_\beta}{s V'^2_\alpha V'^2_\beta} \tag{12}$$

Where ω_{FLL} is the FLL frequency estimation, K_{FLL} is a tunable gain term, V_e is the error between the input voltage signal and the filtered voltage signal, V'_α is the filtered voltage signal and V'_β is the quadrature filtered voltage signal.

The other components are standard for traditional current control and are only discussed briefly here. A phase locked loop (PLL) is used to provide the frequency to the park transforms allowing the transition from the stationary to the synchronous reference frame. This is due to each synchronisation method providing a small error when not acting in the correct respective frame. The FLL acts in the stationary frame while the PLL operates in the synchronous frame. The control system is a contribution from the authors previous work that has been extensively tested and a full description can be found in [8]. Moreover, stability analysis of similar grid side single-phase control topologies has been conducted [39].

B. Train-Side Controller

The train-side converter controller synthesises the three-phase voltage required to drive the electrical machine. A mechanical model of the train employed considering the train linear and rotational inertia and various retarding forces via the Davis equation [40]. The multiple traction motors are lumped into a

Fig. 8.   Train-side converter control and mechanical model.

single machine with equivalent impedance. A system diagram is provided in Fig. 8.

From Fig. 8, a simple gear ratio of 8 is used between the wheel and motor to allow the train to run at HS. Translation from linear to rotational dynamics is completed using a wheel diameter of 1 m. The rotational inertias are lumped and considered as a mass factor, ϕ, as discussed in II.C. The electromagnetic torque is converted to a driving force from which the retarding force calculated from the Davis equation is subtracted. The equivalent mass is then used to determine the train acceleration, velocity and the rotational speed of the machine [32]. The driving force of the train, F_t, is calculated as:

$$F_t = \frac{T_e G}{r_w} - F_R \tag{13}$$

Where F_R is the retarding force acting on the train, T_e is the machine electromagnetic torque, G is the motor to wheel gear ratio and r_w is the train wheel radius. The driving force is then used to calculate the mechanical speed input to the machine:

$$\frac{d\omega_m}{dt} = \frac{GF_t}{m_{te}r_w} \tag{14}$$

Where ω_m is the mechanical speed of the machine and m_{te} is the equivalent mass of the train accounting for rotational inertia. Note that the train is considered a rigid mass and the suspension is disregarded.

The q-axis current reference for the machine is provided via a speed controller. Park transforms are used to move between the stationary and synchronous reference frames with an exact measure of machine speed. The frequency regulation provides a current command based on the filtered derivative of the FLL frequency from the grid-side controller.

$$I_{qfr} = \frac{\omega_{FLL} K_d s}{N s + 1} \tag{15}$$

Where I_{qfr} is the q-axis frequency response current command, ω_{FLL} is the FLL frequency, K_d is the derivative gain and N is a filter constant. In addition to the filtered derivative the FLL frequency may also require a first-order pre-filter if the network provides excessive noise. The stability and performance of the system is extremely sensitive to the filter and inertia parameters. To reduce this effect, processing is used to force the current to follow a fixed envelope after the initial injection

[41], reducing the noise fed back into the system. The envelope provides a decreasing injection of current to generate a linear decrease in train speed. When the controller detects a frequency event the speed controller is turned off to prevent the train from attempting to accelerate. A dead band is added to the loop to make the train respond to large frequency events only. The goal of provided response is to avoid extreme frequency events that activate failsafe systems such as LFDD. This occurs at 48.8 Hz to ensure the frequency is held above 47.5 Hz [42]. Therefore, a large frequency event in this work is defined as greater that 1% of the nominal value (0.5 Hz). Additionally, the railway normal operating conditions are between 49-51 Hz, and should be able to remain connected as low as 47 Hz by reducing performance [1]. Therefore, this value prevents new operating criteria being required and provides a large enough buffer for the system to provide support before LFDD begins. Moreover, the control is limited to respond to frequency drops only, the system will never increase the train speed to burn excess energy. Due to this, a rate limiter can be used to prevent the power injection from decaying too quickly after the initial drop.

An exit strategy is required to ensure the simultaneous reenergization of all trains does not cause a second frequency dip. When the event finishes the trains hold at the lower speed consuming only a small volume of power before a command is made to allow acceleration back to the previous operating speed. Additionally, the power contribution from railways under the present control topology reduces as the event progresses. This further reduces the likelihood of large swings in active power when the trains stop providing energy. The reenergization of the trains can be staggered either manually or automatically, to avoid a sudden connection of load to the system. The order of connection should likely be based on service disruption to ensure the most delayed customers return to speed first.

V. CASE STUDIES

The main goal of this article is to identify the volume of resource available to instigate further research into the proposed idea. However, the operation of the suggested control scheme and the effect the resource may have on the wider network is provided in this section. Two studies are presented to facilitate this. The first verifies that the method presented is possible by providing time domain simulations of a single train responding to a frequency event. The second investigates the role the trains could have played during the 9th of August power cut.

A. Control System Validation

The goal of this study was to verify that the proposed system could deliver the required power quickly without slowing the train to a stop or causing passenger discomfort. This would mean delivering as much power within 100 ms of the event beginning to provide the largest inertia. A balance between IS and FS is achieved by providing a large initial peak limited by the converter rating, followed by a sustained response that decays with time. The train is modelled in Simulink based on the parameters in Table II and a list of further simulation parameters is provided in Table III. Initially, the train is running at 200 km/h consuming 400 kW to balance the retarding forces acting on the

TABLE III
SIMULATION PARAMETERS

Parameter	Symbol	Value
Grid Voltage ($V_{L-L,RMS}$)	V_G	690 V
Converter Power	P_C	5.1 MW
Grid Frequency	ω_G	50 Hz
Grid Impedance	$R_g + jX_g$	0.16+j15.9 $m\Omega$
Filter Impedance	$R_c + jX_c$	1.6+j23.8 $m\Omega$
DC Link Capacitor	C_{DC}	400 mF
Machine Stator Impedance	$R_s + jX_s$	0.69+j51 $m\Omega$
Machine Pole Pairs	p	2
Machine Flux Linkage	F	2
Grid Side Controller		
Current Cont. PI Gains	Kp_{ig}, Ki_{ig}	0.025, 0.53
DC Link Cont. PI Gains	Kp_{DC}, Ki_{DC}	40, 400
PLL PI Gains	Kp_{PLL}, Ki_{PL}	0.911, 202.3
Machine side Controller		
Current Cont. PI Gains	Kp_{im}, Ki_{im}	2, 5
Speed Cont. PI Gains	Kp_n, Ki_n	2000, 2000
Inertia Constant	K_d	120
Filter Constant	N	500
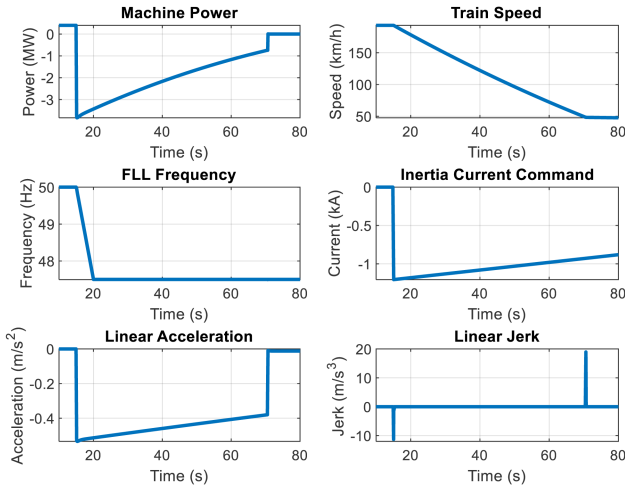
Fig. 9. System responses to a network frequency deviation.

train determined from the Davis equation. A frequency ramp of 0.5 Hz/s was applied to the system and the responses are provided in Fig. 9.

The frequency event begins with a 0.5 Hz/s ramp at 15 seconds. The train quickly begins to slow at a starting rate of around 0.5 ms^{-2} providing almost 4 MW of power within 100 ms and almost 90% of this within the 100 ms limit. This is achieved with the inertia current command from the frequency response block providing a deviation of 1.2 kA which does not exceed the converter limit. The train speed falls from 200 km/h to 50 km/h over the course of a minute. If it is assumed that the train remains at 50 km/h for five minutes while the system recovers, the train would have travelled 12 km less than at normal speed. Factoring in time to accelerate back to 200 km/h the train

would be delayed by approximately 4.5 minutes. This is much smaller than the delays incurred if the event results in the train network being disconnected. Therefore, it is suggested that all trains running above the cut-in speed should respond to large frequency events regardless of the train schedule.

The inertia current command remains large after the train has reached the cut-out speed, but a switch prevents this being followed and the train continues to coast. The jerk at the beginning of the event has a magnitude of around 12 ms^{-3} which is acceptable considering the low acceleration and rigid train model [31]. The higher jerk at the end of the event could be reduced with a smoother handover from inertia control back to speed control. The train does not provide constant power during the event in this case due to the linear deceleration. This can be adapted within the frequency response loop but reduces the volume of initial inertia available. The goal of this study was to push as much power as possible within the inertia time limit as this is likely to provide the highest rate of jerk. The jerk is determined in post-processing to avoid simulation artifacts that occur when chaining multiple derivatives.

B. 9th August Event

The power-cut in the U.K. on the 9th August 2019 saw 1.1 million consumers lose connection to the grid; A large percentage of which were rail passengers. A lightning strike caused a single-phase fault subsequently disconnecting Hornsea One windfarm and a gas power station causing significant loss of generation. Simultaneously, roughly 150 MW of smaller distributed generation also went offline [1]. Due to lack of back-up power generation the LFDD load-shedding scheme was activated. Large parts of the system were restored within 45 minutes, but the failure could have been avoided with a larger supply of emergency backup power. This article has shown that U.K. train network represents a significant energy store available for emergency use.

To investigate the effect that rail services could have had on the 9th of August event a single bus model of the U.K. power network is utilised. The model was developed in DigSILENT PowerFactory [43] and has been validated in [44]. The model has been used previously by the U.K. ESO in a report assessing the system wide inertia and frequency response [45]. The report states that the single busbar, lumped machine model was of adequate complexity to investigate system wide synthetic inertia and primary frequency response requirements. Local and distributed effects are disregarded and should be investigated more carefully. An illustration of the single bus model is provided in Fig. 10.

The loss of generation due to various events in the 60 seconds post lightning strike are included via timed relays. The trains are represented as a single lumped 500 MW source. A second-order transfer function was created to simulate the response shape of the train to frequency deviations:

$$\frac{13.51\,s - 0.0074}{s^2 + 8.03\,s + 0.15} \qquad (16)$$

The transfer function was fitted utilising system identification on the power response shape from Fig. 9 and scaled to provide
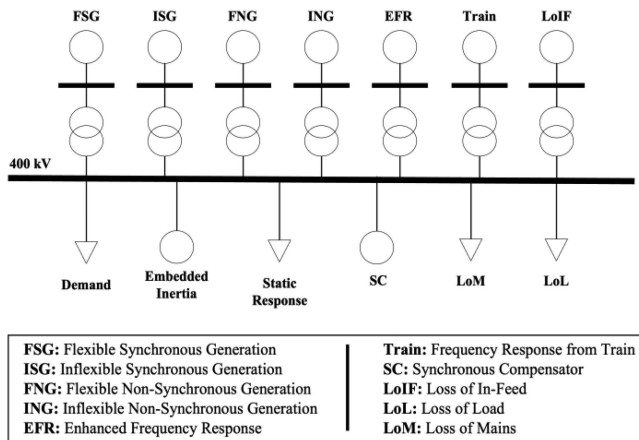
Fig. 10.   Single Bus Model.
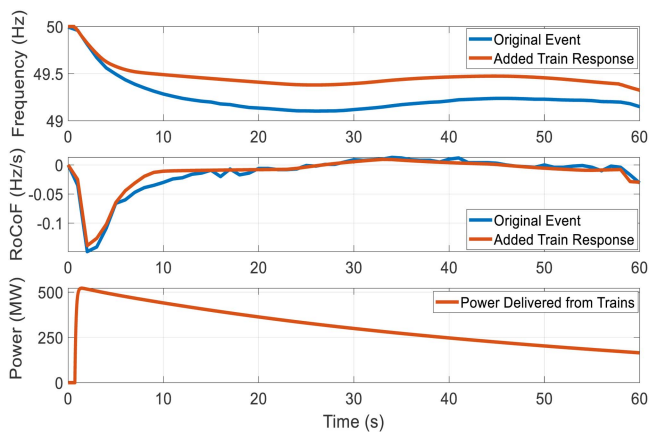
Fig. 11.   Investigation of the 9th of August power-cut.

a peak inertia of 500 MW. This is in line with the analysis conducted in Section II by providing a peak inertia response then a reducing frequency response for a further 60 seconds. The frequency, rate of change of frequency (RoCoF) and train power input are shown in Fig. 11.

From Fig. 11, the original event frequency and RoCoF are shown in blue with the simulated event including the train response shown in orange. The initial RoCoF is similar in both cases with the introduction of the train response slightly reducing the minimum value. The biggest difference occurs in the 5-10 second region where the RoCoF is reduced. This leads to the initial minimum frequency of 49.1 Hz being increased to 49.37 Hz with the inclusion of trains. This proves that the U.K. trains can play a significant role in supporting the network.

VI. CONCLUSION

The U.K. rail network is a significant store of kinetic energy that could be utilised in emergencies to support the electricity network. The volume of power ranges from around 80 MW to 400 MW for a 60 s frequency response and as much as 550 MW for inertia response. The service can be classified as inertia or primary frequency response that prevents a blackout

in the minutes directly following an event. This would provide sufficient time for secondary and tertiary frequency response schemes to activate and rebalance the network. The response available is dependent on number of services running, train speeds, maximum speed deviation and train-cut in speed. As the rail industry becomes increasingly electrified it is expected that the stated values could increase by as much as 100%. Based on the conclusions of this article further work should focus on load flow or time domain simulations of the wider network including traction substations. This research should account for non-linearities and uncertainties to provide increased robustness to the studies. Increased data on the U.K. railway network would be required as a probabilistic approach is harder to implement.

While only the GB network is explored in this article, the idea is extendable to any rail network employing AC EMU's interfaced through a bi-directional converter. Countries employing a higher proportion of high-speed rail with more efficient locomotives such as France, Spain, Germany, China and Japan would possess a larger store of energy [46]. A prospective control scheme has been presented proving the viability of the system. Moreover, the effect that the trains could have had on the 9th of August power cut has been presented. The inclusion of response from the rail network significantly slowed RoCoF and resulted in a smaller frequency deviation.

REFERENCES

[1] S. Wilde, OFGEM, "9th August 2019 power outage report," OFGEM, London, Jan. 2020.

[2] C. Maciver, K. Bell, and M. Nedd, "An analysis of the August 9th 2019 GB transmission system frequency incident," *Electric Power Syst. Res.*, vol. 199, 2021, Art. no. 107444, doi: 10.1016/j.epsr.2021.107444.

[3] F. Milano, F. Dorfler, G. Hug, J. Hill, and G. Verbic, "Foundations and challenges of low-inertia systems," in *Proc. Power Syst. Computation Conf. Dublin*, 2018, pp. 1–25.

[4] Q. Hong, M. Asif Uddin Khan, C. Henderson, A. Egea-Àlvarez, D. Tzelepis, and C. Booth, "Addressing frequency control challenges in future low-inertia power systems: A Great Britain perspective," *Engineering*, vol. 7, pp. 1057–1063, 2021, doi: 10.1016/j.eng.2021.06.005.

[5] H. Gu, R. Yan, and T. Saha, "Review of system strength and inertia requirements for the national electricity market of Australia," *CSEE J. Power Energy Syst.*, vol. 5, no. 3, pp. 295–305, Sep. 2019, doi: 10.17775/CSEE-JPES.2019.00230.

[6] J. Alipoor, Y. Miura, and T. Ise, "Power system stabilization using virtual synchronous generator with alternating moment of inertia," *IEEE J. Emerg. Sel. Topics Power Electron.*, vol. 3, no. 2, pp. 451–458, Jan. 2015.

[7] G. Magdy, H. Ali, and D. Xu, "A new synthetic inertia system based on electric vehicles to support the frequency stability of low-inertia modern power grids," *J. Cleaner Prod.*, vol. 297, 2021, Art. no. 126595, doi: 10.1016/j.jclepro.2021.126595.

[8] C. Henderson, N. McNeill, G. Wu, D. Holliday, and A. Egea-Àlvarez, "Vector control of a single-phase voltage source converter for the supply of inertia to weak grids," in *Proc. IEEE 10th Int. Conf. Power Electron., Mach. Drives*, 2020, pp. 615–620.

[9] A. Roscoe et al., "Response of a grid forming wind farm to system events, and the impact of external and internal damping," *IET Renewable Power Gener.*, vol. 14, no. 19, pp. 3908–3917, 2020, doi: 10.1049/iet-rpg.2020.0638.

[10] J. Morren, S. W. H. De Haan, W. L. Kling, and J. A. Ferreira, "Wind turbines emulating inertia and supporting primary frequency control," *IEEE Trans. Power Syst.*, vol. 21, no. 1, pp. 433–434, Feb. 2006, doi: 10.1109/tp-wrs.2005.861956.

[11] National Grid ESO, "Operability strategy report," *System Operability Framework 2021*, 2021.

[12] M. Brenna, F. Foiadelli, and D. Zaninelli, *Electrical Railway Transportation Systems*. Piscataway, NJ, USA: Wiley-IEEE Press, 2018.

[13] International Electrotechnical Commission, *Railway applications - Fixed installations - Traction transformers*, Standard IEC 62695:2014, Geneva, Switzerland, 2014.

[14] British Standards, *Railway Applications. Fixed Installations. Traction Transformers*, Standard BS EN 50329:2003+A1:2010, U. K., 2006.

[15] British Standards, *Railway Applications. Power Supply and Rolling Stock. Technical Criteria for the Coordination Between Power Supply (Substation) and Rolling Stock to Achieve Interoperability*, Standard BS EN 50388:2012, U. K., 2013.

[16] G. Theeg and S. Vlasenko, *Railway Signalling & Interlocking: International Compendium*. Hamburg, Germany: Eurail-Press Publications, 2009.

[17] F. Ciccarelli, M. Fantauzzi, D. Lauria, and R. Rizzo, "Special transformers arrangement for AC railway systems," in *Proc. IEEE Elect. Syst. for Aircr., Railway Ship Propulsion*, 2012, pp. 1–6.

[18] H.Y. Kuo and T. H. Chen, "Rigorous evaluation of the voltage unbalance due to high-speed railway demands," *IEEE Trans. Veh. Technol.*, vol. 47, no. 4, pp. 1385–1389, Nov. 1998, doi: 10.1109/25.728533.

[19] M. Kalantari, M. J. Sadeghi, S. S. Fazel, and S. Farshad, "Investigation of power factor behavior in AC railway system based on special traction transformers," *J. Electromagn. Anal. Appl.*, vol. 2, no. 11, pp. 618–626, 2010, doi: 10.4236/jemaa.2010.211081.

[20] B. K. Chen and B. S. Guo, "Three phase models of specially connected transformers," *IEEE Trans. Power Del.*, vol. 11, no. 1, pp. 323–330, Jan. 1996, doi: 10.1109/61.484031.

[21] Q. Xu et al., "Analysis and comparison of modular railway power conditioner for high-speed railway traction system," *IEEE Trans. Power Electron.*, vol. 32, no. 8, pp. 6031–6048, Aug. 2017, doi: 10.1109/tpel.2016.2616721.

[22] Z. Zhang, B. Wu, J. Kang, and L. Luo, "A multi-purpose balanced transformer for railway traction applications," *IEEE Trans. Power Del.*, vol. 24, no. 2, pp. 711–718, Apr. 2009, doi: 10.1109/tpwrd.2008.2008491.

[23] M. F. M. Arani, Y. A.-R. I. Mohamed, and E. F. El-Saadany, "Analysis and mitigation of the impacts of asymmetrical virtual inertia," *IEEE Trans. Power Syst.*, vol. 29, no. 6, pp. 2862–2874, Nov. 2014, doi: 10.1109/tpwrs.2014.2309675.

[24] E. Sareen, Network Rail, "Periodic review 2013: Network rail consultation on traction electricity & electrification asset usage charges in CP5," *Netw. Rail*, London, Sep. 2012.

[25] Office of Rail and Road U.K. Gov., "Rail infrastructure and assests 2020-21," Oct. 14, 2021. [Online]. Available: https://dataportal.orr.gov.uk/media/2014/rail-infrastructure-assets-2020-21.pdf

[26] J. Zhang, W. Liu, R. Zhou, Y. Zhang, Y. Li, and J. He, "Modeling and analysis of DC traction power supply system based on bi-directional converter device," in *Proc. IEEE Veh. Power Propulsion Conf.*, 2019, pp. 1–6.

[27] Network Rail, Network Rail Data Feeds, 2022. [Online]. Available: https://datafeeds.networkrail.co.uk

[28] U.K. Govt. Department for Transport, "Rolling stock perspective second edition," London, U.K., 2016.

[29] European Commission, *Study On The Prices and Quality of Rail Passenger Services*. Brussels, 2016.

[30] National Grid ESO, "NOA stability pathfinder phase 3 technical performance requirements," Aug. 2021. [Online]. Available: https://www.nationalgrideso.com/document/208351/download

[31] J. P. Powell and R. Palacín, "Passenger stability within moving railway vehicles: Limits on maximum longitudinal acceleration," *Urban Rail Transit*, vol. 1, no. 2, pp. 95–103, 2015, doi: 10.1007/s40864-015-0012-y.

[32] R. Watson, "Factors influencing the energy consumption of high speed rail and comparisons with other modes," Ph.D., Dept. Mech. Eng., Imperial College, London, U.K., 2012.

[33] D. M. Greenwood, K. Y. Lim, C. Patsios, P. F. Lyons, Y. S. Lim, and P. C. Taylor, "Frequency response services designed for energy storage," *Appl. Energy*, vol. 203, pp. 115–127, 2017, doi: 10.1016/j.apenergy.2017.06.046.

[34] National Grid ESO, "Mandatory frequency response," 2021. [Online] Available: https://www.nationalgrideso.com/balancing-services/mandatory-response-services?overview

[35] C. G. Maggs, *The Birmingham to Gloucester Line*. Stroud, U.K.: Amberley, 2013.

[36] N. Nimpitiwan, G. T. Heydt, R. Ayyanar, and S. Suryanarayanan, "Fault current contribution from synchronous machine and inverter based distributed generators," *IEEE Trans. Power Del.*, vol. 22, no. 1, pp. 634–641, Jan. 2007, doi: 10.1109/tpwrd.2006.881440.

[37] High Speed Two Ltd., "Phase one: London to west midlands," 2022. Accessed: 2022. [Online]. Available: https://www.hs2.org.uk/what-is-hs2/phase-one-london-west-midlands/

[38] S. Danielsen, O. B. Fosso, M. Molinas, J. A. Suul, and T. Toftevaag, "Simplified models of a single-phase power electronic inverter for railway power system stability analysis—Development and evaluation," *Electric Power Syst. Res.*, vol. 80, no. 2, pp. 204–214, 2010, doi: 10.1016/j.epsr.2009.09.003.

[39] Y. Liao, Z. Liu, H. Zhang, and B. Wen, "Low-frequency stability analysis of single-phase system with *dq*-frame impedance approach—Part I: Impedance modeling and verification," *IEEE Trans. Ind. Appl.*, vol. 54, no. 5, pp. 4999–5011, Sep./Oct. 2018, doi: 10.1109/tia.2018.2832027.

[40] B. P. Rochard and F. Schmid, "A review of methods to measure and calculate train resistances," *Proc. Inst. Mech. Engineers, Part F: J. Rail Rapid Transit*, vol. 214, no. 4, pp. 185–199, 2000, doi: 10.1243/0954409001531306.

[41] A. Cooke, D. Strickland, and K. Forkasiewicz, "Energy storage for enhanced frequency response services," in *Proc. 52nd Int. Universities Power Eng. Conf.*, 2017, pp. 1–6, doi: 10.1109/UPEC.2017.8231914.

[42] National grid ESO, "Interim report into the low frequency demand disconnection (LFDD) following generator trips and frequency excursion on 9 Aug 2019," London, Aug. 2019.

[43] DigSILENT, "Power factory," 2022. [Online]. Available: http://www.digsilent.de/index.php/products-powerfactory.html

[44] M. Nedd, W. Bukhsh, C. Maciver, and K. Bell, "Metrics for determining the frequency stability limits of a power system: A GB case study," *Electric Power Syst. Res.*, vol. 190, 2021, Art. no. 106553, doi: 10.1016/j.epsr.2020.106553.

[45] T. Derry, National Grid ESO, "GC022 - Frequency Response," London, Jan. 2013.

[46] Environmental and Energy Study Insitute, *High Speed Rail Development Worldwide*, 2018.